ACS Catalysis

pubs.acs.org/acscatalysis Letter

Atmosphere-Pressure Methane Oxidation to Methyl Trifluoroacetate Enabled by a Porous Organic Polymer-Supported Single-Site Palladium Catalyst

Yiwen Zhang,[⊥] Min Zhang,[⊥] Zhengbo Han, Shijun Huang, Daqiang Yuan,* and Weiping Su*

Cite This: *ACS Catal.* 2021, 11, 1008−1013 Read Online

ABSTRACT: The efficient conversion of methane into methanol at low temperature under low pressure remains a great challenge largely because of the inertness and poor solubility of methane. Herein, we report that a porous organic polymer-supported Pd catalyst, which was constructed via Friedel−Crafts type polymerization between 4,6-dichloropyrimidine and 1,3,5-triphenyl benzene and subsequent metalation, enabled the conversion of methane to methyl trifluoroacetate, a precursor to methanol, under atmosphere pressure (1 atm) at 80 °C to afford a 51% yield relative to methane with a TON of 664 over 20 h. On increasing the pressure to 30 bar, this palladium catalyst offered a TON of 1276 for a run and could be reused for at least five runs without a notable loss of activity. The characterization of this Pd catalyst revealed its good affinity for methane uptake that would increase the concentration of methane in the local space around the Pd center and the homogeneous distribution of Pd^{2+} on support that would protect the catalytically active metal species, shedding light on the high catalytic activity of this Pd catalyst toward methane conversion.

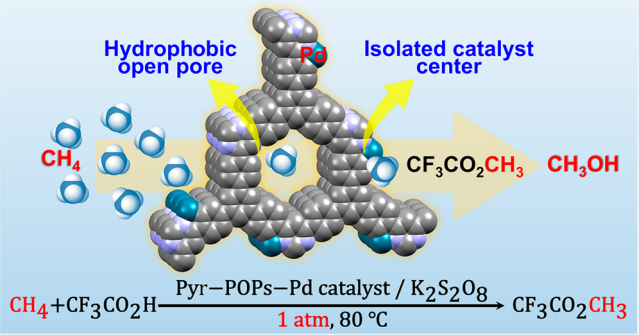

KEYWORDS: *porous organic polymer, methane, oxidation, methyl trifluoroacetate, palladium catalyst*

Methane, the main component of natural gas, is an abundant, inexpensive resource of hydrocarbon.[1−3] So far, practical conversions of methane into synthetic fuels and fine-chemicals have all relied on the high-temperature, high-pressure multistep processes that consist of the initial steam reforming to generate syngas (a mixture of carbon monoxide and hydrogen) and subsequent transformations of syngas to targeted products.[4−6] Over the past decades, the direct conversion of methane to value-added products without the reliance of formation of intermediate syngas under mild conditions (e.g., low-temperature and low-pressure) has been the sought-after goal of chemists from both academic and industrial communities,[7−14] because the achievement of such a goal would provide low-energy, cost-effective processes, and allow realizing the potential utility of widely available methane as an industrial feedstock. As a result, great advances have been achieved in the development of the strategies for addressing the challenges posed by the intrinsic inertness of methane that stems from the strong C−H bond, nonpolarity of the molecule, poor solubility in most solvents, and low acidity.[15−35] Nevertheless, the efficient catalysts for the direct conversion of methane under mild conditions remain in high demand.[12−14]

Realizing that methanol is a versatile feedstock for production of various fine chemicals,[36−38] chemists have devoted great efforts to the development of the catalytic methods for direct conversion of methane to methanol or methanol derivatives via selective oxidation.[14,23−38] These elegant studies have disclosed a variety of factors that are responsible for the catalytic efficiency, including ligand effects on the activity, selectivity and lifetime of catalysts,[27,29,32] the effects of nature and concentration of oxidants on catalysis,[28,30] the dependence of the reaction types on the intrinsic properties of metal catalysts,[26,31,35] and the developed strategy to avoid overoxidation of methanol product.[25] These findings have led to the improvement of the activity and lifetime of catalysts and reaction selectivity, representing significant advances in this area. However, there is still room for the development of a catalyst system to achieve the efficient conversion of methane to methanol under mild conditions, since the existing methods generally require high temperature (up to 200 °C) and high pressure (typically >30 bar). The

Received: November 27, 2020
Revised: December 25, 2020
Published: January 7, 2021

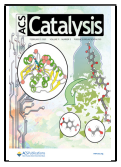

https://dx.doi.org/10.1021/acscatal.0c05205
ACS Catal. 2021, 11, 1008−1013

homogeneous trifluoroacetic acid based systems, which employ highly stable bis(NHC) palladium,[27] manganese oxide,[39] cobalt acetate,[40] or copper oxide[31] as the catalyst, allow the selective oxidation of methane to methyl trifluoroacetate to occur under realtively mild conditions but with a low turnover number (TON).

Recently, metal−organic frameworks (MOFs) as well as porous organic polymers (POPs) have been widely used as versatile and tunable catalyst supports to construct single-site metal catalysts.[21,22,32−35,41−59] The pioneering studies in this area have demonstrated that the separation of metal catalyst within porous frameworks protects highly catalytically active, coordinatively unsaturated metal species from agglomeration and decomposition and therefore endows active catalysts with the high stability that is inaccessible in homogeneous catalysis systems.[22,41,45,46] Importantly, depending on pore size and hydrophilic/hydrophobic nature, MOFs and POPs are capable of selectively adsorbing organic compounds including gaseous substances.[60−62] These achievements inspired us to consider whether MOFs/POPs-supported solid catalysts could realize the direct conversion of methane to methanol under mild conditions. The desired process combines the high activity of homogeneous catalysts and the ease of heterogeneous catalysts and thus would exhibit an excellent overall performance. The potential advantages of the MOFs/POPs-supported solid catalysts for methane conversion, we speculated, lie in the following two aspects. First, the hydrophobic open-pores of MOFs or POPs may adsorb methane gas[60,62] and thus significantly increase the concentration of methane in the local space around the catalyst centers immobilized within pores, which would lead to a decrease in the activation entropy of methane and allow for the reaction under relatively low pressure. Second, the choice of the proper ligand moiety tethered to MOFs or POPs frameworks may give rise to the catalytically active metal catalysts[41] that, in combination with the decreased activation entropy, enable the reaction to occur at relatively low temperatures and extend the lifetimes of catalysts because of the isolation of metal centers of catalysts.[22] Herein, we report a POPs-supported palladium catalyst that enables the oxidative conversion of methane to methyl trifluoroacetate at 80 °C under pressure of 1 atm with the turnover number (TON) of 664 reached over 20 h (Figure 1). To the best of our knowledge, no method for the conversion of methane under such low pressure has been reported before our work. When CH_4 pressure was increased to 30 atm, this reaction obtained a TON of 1276 over 20 h. This POPs-supported palladium catalyst did not show a notable decrease in catalytic activity after being reused at least 5 times in the conversion of methane to methyl trifluoroacetate. Our findings demonstrate the great potential of MOFs/POPs-supported catalysts to affect the challenging conversions of inert gaseous substrates under mild conditions.

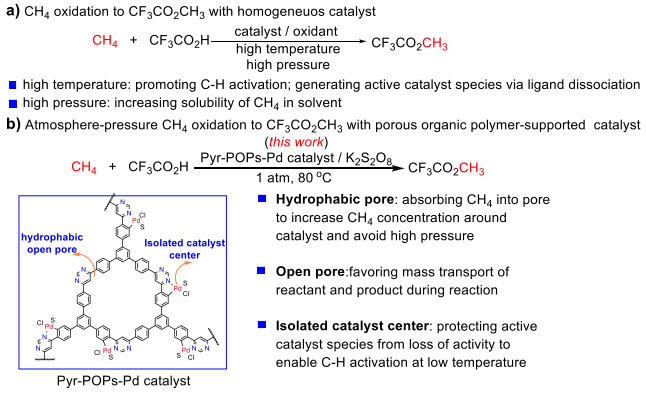

Figure 1. Methane oxidation to methyl trifluoroacetate. (a) Conventional conversion of CH_4 with homogeneous catalysts. (b) Conversion of CH_4 with porous organic catalyst−supported catalyst (this work).

Our investigations began with preparation and characterization of POPs-supported metal catalysts. Recently, a microporous covalent triazine-based organic polymer that is constructed from cross-coupling between 1,3,5-trichloro triazine and 1,3,5-triphenyl benzene, proved to be an adsorbent for CH_4 with pretty good capture capacity.[63] In light of this, we synthesized an analogous POPs material using the method previously established by us[64] to check its utility as catalyst support. As shown in Figure 2, the designed POPs material was prepared via $AlCl_3$-mediated Friedel−Crafts arylation of 4,6-dichloropyrimidine with 1,3,5-triphenyl benzene that was conducted at 40 °C in methylene chloride for 20 h and isolated as a solid powder (denoted as **Pyr-POPs**) after purification (for experimental details, see Supporting Information). Then, **Pyr-POPs** was postsynthetically metalated via nitrogen ligand-assisted cyclopalladation using Na_2PdCl_4 as a palladium source to generate Pd-incorporating porous organic polymer, **Pyr-POPs-Pd**.

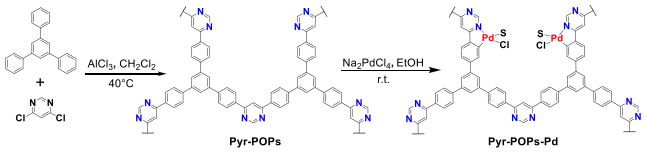

Figure 2. Construction of porous organic polymer incorporating pyrimidine units (**Pyr-POPs**) and palladation of **Pyr-POPs** to **Pyr-POPs-Pd**.

The successful synthesis of **Pyr-POPs** was supported by several structure determination approaches. The solid-state ^{13}C NMR spectrum of **Pyr-POPs** shows the peaks at 169 and 162 ppm that can be assigned to carbon atoms at the pyrimidine ring and the broad peaks at around 139 and 128 ppm corresponding to carbon atoms of phenyl rings, suggesting that both pyrimidine and 1,3,5-triphenyl benzene moieties are incorporated into the **Pyr-POPs** framework (Figure S1). Nevertheless, a peak at 35 ppm in this ^{13}C NMR spectrum reflects the incorporation of methylene carbon into the **Pyr-POPs** due in large part to the $AlCl_3$-mediated Friedel−Crafts alkylation reaction of 1,3,5-triphenyl benzene with methylene chloride solvent, which is consistent with the elemental analysis of **Pyr-POPs** sample that is slightly different from the values calculated on the basis of the expected structure of **Pyr-POPs** (Figure 2). The Fourier-transform infrared (FTIR) spectrum (Figure S2, S3) provides the structural information similar to its ^{13}C NMR spectrum. The bands at 1506 and 1375 cm^{-1} appearing in the spectrum of **Pyr-POPs** may result from the C═N and C−N stretching vibrations of the pyrimidine ring. Besides, the disappearing C−Cl stretching band at 850 cm^{-1} in the FTIR spectrum confirms the complete conversion of pyrimidinyl chloride.[65]

X-ray photoelectron spectroscopy analysis validated that the elemental compositions of **Pyr-POPs-Pd** are C, N, Cl, and Pd

https://dx.doi.org/10.1021/acscatal.0c05205
ACS Catal. 2021, 11, 1008−1013

elements (Figure S4). Moreover, the XPS spectrum of **Pyr-POPs-Pd** revealed that the binding energy peaks at 337.6 and 342.8 eV are characteristic signals of the Pd $3d_{5/2}$ and Pd $3d_{3/2}$ corresponding to Pd^{II} oxidation state (Figure S5). In comparison with the Na_2PdCl_4 (338.1 and 343.3 eV), the Pd^{II} binding energy in the **Pyr-POPs-Pd** shifted negatively by 0.5 eV, which can be attributed to the strong electron-donation of the **Pyr-POPs** framework. These results confirm that the Pd^{II} is successfully immobilized on the **Pyr-POPs** by coordination to pyridine functional groups rather than by physical adsorption of Na_2PdCl_4 on the surface.[66]

The combined TEM/EDX analysis (TEM, transmission electron microscopy; EDX, energy-dispersive X-ray spectroscopy) indicated a very homogeneous palladium loading without detectable palladium clusters or nanoparticles within **Pyr-POPs-Pd** framework. The high-annular dark-field scanning TEM and EDX mapping spectroscopy also supported the uniform inclusion of the carbon, nitrogen, palladium, and chlorine center into the polymer frameworks (Figure S6). Bright spots marked with red circles in the aberration-corrected HAADF-STEM image (Figure S8) arose from isolated atoms, which indicated that the agglomeration of Pd(II) ions might not occur during the impregnation step. A broad peak centered around 20° in the powder X-ray diffraction pattern (Figure S9) indicates the amorphous character of the **Pyr-POPs** and **Pyr-POPs-Pd** material that consists of particles with sizes ranging from 10 to 30 μm as shown by the field-emission scanning electron microscopy image (Figure S10).

The nitrogen sorption measurements demonstrate microporous structures of **Pyr-POPs-Pd** and **Pyr-POPs** samples. As shown in Figure 3a, both the samples display a classical type I isotherm with a sharp uptake at low relative pressure ($P/P°$< 0.1), reflecting abundant micropores in frameworks of **Pyr-POPs-Pd** and **Pyr-POPs**. Actually, the micropores of suitable size in heterogeneous catalysts are beneficial to mass transport for reactants and products during catalysis process. **Pyr-POPs** is shown to have an N_2 uptake of 325 cm^3g^{-1} with a Brunauer−Emmett−Teller (BET) surface area of 812 m^2g^{-1} (pore volume 0.50 cm^3 g^{-1}), while **Pyr-POPs-Pd** demonstrates a smaller N_2 uptake of 248 cm^3g^{-1} with a BET surface area of 671 m^2g^{-1} (pore volume 0.37 cm^3 g^{-1}). The pore-size distributions were calculated by the density functional theory model (Figure 3a, inset). On the basis of these calculations, **Pyr-POPs-Pd** was revealed to have two types of micropores with pore widths of 0.54 and 0.64 nm, which are smaller than those of **Pyr-POPs** with pore widths of 0.68 and 0.79 nm as a result of incorporation of Pd species into **Pyr-POPs** porous framework. Importantly, **Pyr-POPs** and **Pyr-POPs-Pd** exhibit a good affinity for CH_4 with CH_4 uptake of 29.4 and 23.4 cm^3g^{-1} at 273 K, 25.0 and 19.4 cm^3g^{-1} at 283 K, and 20.6 and 15.9 cm^3g^{-1} at 293 K, respectively (Figure 3b,c). To probe the host-CH_4 binding affinity, the isosteric heats of adsorption (Q_{st}) are calculated on the basis of the CH_4-adsorption isotherms at 273, 283, and 293 K (Figure 3d). The high Q_{st} values derived from these data point to the good affinity between CH_4 and the hydrophobic walls of micropores.

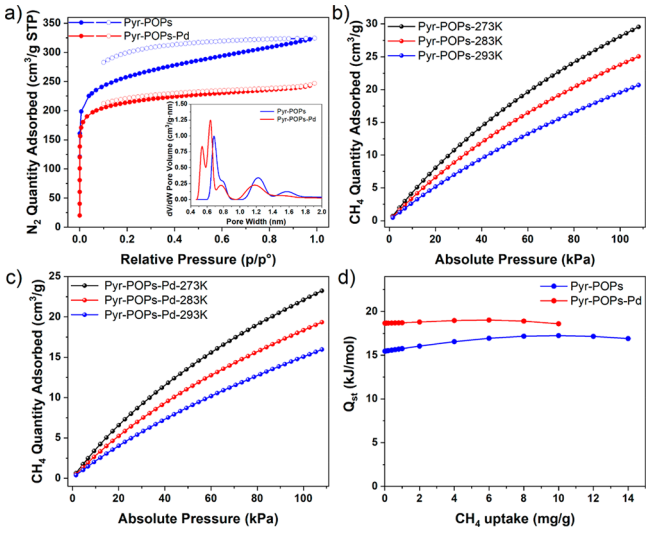

Figure 3. (a) Nitrogen sorption isotherms of **Pyr-POPs** and **Pyr-POPs-Pd** measured at 77 K. Inset: Pore size distributions of **Pyr-POPs** (blue) and **Pyr-POPs-Pd** (red). (b, c) CH_4 adsorption isotherms of **Pyr-POPs** (b) and **Pyr-POPs-Pd** (c) collected at 273, 283, and 293 K. (d) Heats of CH_4 adsorption for **Pyr-POPs** and **Pyr-POPs-Pd** at 273, 283, and 293 K.

With Pd-incorporating porous organic polymer **Pyr-POPs-Pd** in hand, we evaluated the catalytic activity of **Pyr-POPs-Pd** toward the direct conversion of methane under mild conditions using the selective oxidation of methane to generate methyl trifluoroacetate as a model system (Table 1). The model reaction was carried out in a mixed solvent of trifluoroacetic acid and trifluoroacetic acid anhydride at 80 °C for 20 h under the indicated CH_4 pressure using $K_2S_2O_8$ as an oxidant and an autoclave as a reactor. To our delight, 1 mg of **Pyr-POPs-Pd** with 5.95 wt % palladium content was observed to be a high active catalyst for the conversion of methane to methyl trifluoroacetate under 30 bar of CH_4 pressure, affording a TON as high as 1276 (entry 1). Interestingly, this porous framework-supported Pd catalyst enabled the reaction to take place under atmosphere pressure (1 atm) in a 51% yield relative to CH_4 with a TON of 664 (entry 2). To evaluate the effect of porous framework support on the catalytic activity of the catalyst, a molecular bimetallic palladium complex, which is similar in the coordination sphere of palladium center to **Pyr-POPs-Pd**, was tested as a catalyst for the model reaction under 30 bar of CH_4 pressure (entry 3). This chloride-bridged bimetallic palladium complex bearing a

Table 1. Effects of Reaction Parameters on the Catalytic Efficiency of the CH_4 Oxidation to Methyl Trifluoroacetate[a]

$$CH_4 + CF_3CO_2H \xrightarrow[\text{TFA / (TFA)}_2\text{O, 80 °C, 20 h}]{\text{Catalyst / K}_2\text{S}_2\text{O}_8} CF_3CO_2CH_3$$

entry	catalyst	methane (bar)	CF_3CO_2Me (mM)	TON[b]
1	Pyr-POPs-Pd	30	102.14	1276
2	Pyr-POPs-Pd	1	53.14	664[c]
3	$[Pd(2\text{-PhPy})(\mu\text{-Cl})]_2$[d]	30	13.33	167
4	Na_2PdCl_4[e]	30	26.25	328
5	Na_2PdCl_4[e]+Pyr-POPs	30	45.36	567

[a]Reaction conditions: 1 mg of catalyst with 5.95 wt % Pd content, 570 mg of $K_2S_2O_8$(2.1 mmol), 6 mL of TFA, 1 mL of $(TFA)_2O$, 20 h, 80 °C, under the indicated CH_4 pressure (25 °C). [b]TON was calculated as the molar ratio of CF_3CO_2Me to the palladium content. [c]51% yield based on methane was obtained as methane (0.73 mmol) is the limiting reagent under atmosphere pressure. [d]0.28 μmol catalyst. [e]10 μL stock solution of $NaPdCl_4$ in H_2O (0.056 M).

https://dx.doi.org/10.1021/acscatal.0c05205
ACS Catal. 2021, 11, 1008−1013

cyclopalladated 2-phenylpyridine ligand was observed to promote the reaction but offer a much lower TON (167) than **Pyr-POPs-Pd**, illustrating the positive effect of porous framework support **Pyr-POPs**. $NaPdCl_4$ also effected the conversion of methane with a TON of 328 (entry 4), while introduction of **Pyr-POPs** into the reaction system with $NaPdCl_4$ to *in situ* generate the **Pyr-POPs-Pd** led to the improvement of TON (576) (entry 5), once again indicating the positive role of **Pyr-POPs** in the enhancement of catalyst activity. The significantly decreased TON value with *in situ* generation of **Pyr-POPs-Pd** compared with the case of presynthesized **Pyr-POPs-Pd** is likely due to incomplete incorporation of Pd salts into **POPs** framework.

The insight into the mechanism for this direct conversion of methane was obtained by the free-radical trapping experiment in which introducing radical scavengers such as benzophenone, hydroquinone, and phenol into the reaction system shut down the reaction of methane. This radical trapping experiment suggested the reaction involved formation of free-radical intermediate. Next, the recyclability of this heterogeneous catalyst **Pyr-POPs-Pd** was investigated (Figure 4). The used

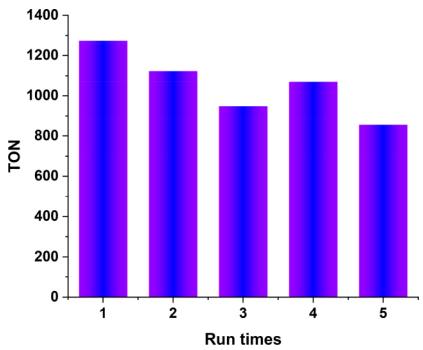

Figure 4. Evaluation of the recyclability of **Pyr-POPs-Pd** catalyst in the CH_4 oxidation to methyl trifluoroacetate. All reactions were conducted under the conditions similar to those described in Table 1, entry1.

Pyr-POPs-Pd catalyst, which was isolated from the first-run reaction system by centrifugation and filtration and subsequently purified by washing with water and ketone, was found to be still active toward the conversion of methane to methyl trifluoroacetate under the standard reaction conditions. This **Pyr-POPs-Pd** catalyst proved to be reusable for at least five iterative runs without notable loss of activity, highlighting its stability against decomposition under acidic conditions. We carried out TEM images, HAADF-STEM image, EDS elemental mapping spectroscopy (Figure S11) as well as aberration-corrected HAADF-STEM image (Figure S13) of recycled catalyst, and it can be seen that the metal palladium in recovered catalyst is stable. Moreover, the solid-phase ^{13}C NMR spectra of recyclable catalyst were mostly maintained (Figure S14). These observations suggest that the stability and structural integrity of the Pyr-POPs-Pd catalyst could withstand the test, thus providing potential to practical application.

In summary, we have synthesized a single-site palladium catalyst supported on porous organic polymers framework that features microporous structure, high BET surface area, and good affinity for methane uptake. This porous organic polymer-supported single-site palladium heterogeneous catalysts **Pyr-POPs-Pd** proved to be active toward the direct conversion of methane under mild conditions, as exemplified by the **Pyr-POPs-Pd** enabled selective oxidation of methane by $K_2S_2O_8$ under atmosphere pressure (1 atm) that offered methyl trifluoroacetate in a 51% yield relative to CH_4 with a TON of 664. When pressure was increased to 30 bar, **Pyr-POPs-Pd** provided a TON as high as 1276 and could be reused for at least 5 runs without significant loss of activity, indicative of its good stability. The observation that **Pyr-POPs-Pd** outperformed the molecular palladium complex with similar coordination sphere in terms of both catalytic efficiency and reaction conditions implicates that the ability of porous framework to adsorb methane and the isolation of Pd centers within **Pyr-POPs-Pd** may both play key roles in enhancement of its catalytic activity. On the basis of the tunability of porosity, chirality, hydrophilic/hydrophobic nature and chemical functionality of porous frameworks, the design and development of porous framework-supported metal catalysts for efficient chemical conversions, particularly with inert but readily available starting materials is underway in our laboratories.

■ ASSOCIATED CONTENT

Supporting Information

The Supporting Information is available free of charge at https://pubs.acs.org/doi/10.1021/acscatal.0c05205.

Synthesis and characterizations for **Pyr-POPs** and **Pyr-POPs-Pd**, detailed procedures, and characterizations data of catalytic methane oxidation (PDF)

■ AUTHOR INFORMATION

Corresponding Authors

Daqiang Yuan − *State Key Laboratory of Structural Chemistry, Fujian Institute of Research on the Structure of Matter, Chinese Academy of Sciences, Fuzhou 350002, China; University of the Chinese Academy of Sciences, Beijing 100049, China;* orcid.org/0000-0003-4627-072X; Email: ydq@fjirsm.ac.cn

Weiping Su − *State Key Laboratory of Structural Chemistry, Fujian Institute of Research on the Structure of Matter, Chinese Academy of Sciences, Fuzhou 350002, China; University of the Chinese Academy of Sciences, Beijing 100049, China;* orcid.org/0000-0001-5695-6333; Email: wpsu@fjirsm.ac.cn

Authors

Yiwen Zhang − *State Key Laboratory of Structural Chemistry, Fujian Institute of Research on the Structure of Matter, Chinese Academy of Sciences, Fuzhou 350002, China; College of Chemistry, Liaoning University, Shenyang 110036, China*

Min Zhang − *State Key Laboratory of Structural Chemistry, Fujian Institute of Research on the Structure of Matter, Chinese Academy of Sciences, Fuzhou 350002, China;* orcid.org/0000-0002-4344-9815

Zhengbo Han − *College of Chemistry, Liaoning University, Shenyang 110036, China;* orcid.org/0000-0001-8635-9783

Shijun Huang − *State Key Laboratory of Structural Chemistry, Fujian Institute of Research on the Structure of Matter, Chinese Academy of Sciences, Fuzhou 350002, China*

Complete contact information is available at: https://pubs.acs.org/10.1021/acscatal.0c05205

https://dx.doi.org/10.1021/acscatal.0c05205
ACS Catal. 2021, 11, 1008−1013

Author Contributions

⊥(Y.Z., M.Z.) These authors contributed equally.

Notes

The authors declare no competing financial interest.

■ ACKNOWLEDGMENTS

This work was supported by the National Key Research and Development Program of China (2018YFA0704502), the National Natural Science Foundation of China (Grants No. 21931011, 22071241, and u1505242), the Strategic Priority Research Program of the Chinese Academy of Sciences (XDB20000000 and XDB10040304), and the Key Research Program of Frontier Sciences, CAS (QYZDJ-SSW-SLH024).

■ REFERENCES

(1) Kerr, R. A. Energy. Natural gas from shale bursts onto the scene. *Science* **2010**, *328*, 1624−1626.

(2) Caballero, A.; Perez, P. J. Methane as raw material in synthetic chemistry: the final frontier. *Chem. Soc. Rev.* **2013**, *42*, 8809−8820.

(3) Saha, D.; Grappe, H. A.; Chakraborty, A.; Orkoulas, G. Postextraction separation, on-board storage, and catalytic conversion of methane in natural gas: a review. *Chem. Rev.* **2016**, *116*, 11436−11499.

(4) Rostrup-Nielsen, J. R.; Sehested, J.; Nørskov, J. K. Hydrogen and synthesis gas by steam- and CO_2 reforming. *Adv. Catal.* **2002**, *47*, 65−139.

(5) Alvarez-Galvan, M. C.; Mota, N.; Ojeda, M.; Rojas, S.; Navarro, R. M.; Fierro, J. L. G. Direct methane conversion routes to chemicals and fuels. *Catal. Today* **2011**, *171*, 15−23.

(6) Wang, B.; Albarracín-Suazo, S.; Pagán-Torres, Y.; Nikolla, E. Advances in methane conversion processes. *Catal. Today* **2017**, *285*, 147−158.

(7) Crabtree, R. H. Aspects of methane chemistry. *Chem. Rev.* **1995**, *95*, 987−1007.

(8) Shilov, A. E.; Shul'pin, G. B. Activation of C−H bonds by metal complexes. *Chem. Rev.* **1997**, *97*, 2879−2932.

(9) Lunsford, J. H. Catalytic conversion of methane to more useful chemicals and fuels: a challenge for the 21st century. *Catal. Today* **2000**, *63*, 165−174.

(10) Tang, P.; Zhu, Q.; Wu, Z.; Ma, D. Methane activation: the past and future. *Energy Environ. Sci.* **2014**, *7*, 2580−2591.

(11) Hartwig, J. F. Evolution of C-H Bond functionalization from methane to methodology. *J. Am. Chem. Soc.* **2016**, *138*, 2−24.

(12) Schwarz, H. Chemistry with methane: concepts rather than recipes. *Angew. Chem., Int. Ed.* **2011**, *50*, 10096−10115.

(13) Gunsalus, N. J.; Koppaka, A.; Park, S. H.; Bischof, S. M.; Hashiguchi, B. G.; Periana, R. A. Homogeneous functionalization of methane. *Chem. Rev.* **2017**, *117*, 8521−8573.

(14) Ravi, M.; Ranocchiari, M.; van Bokhoven, J. A. The direct catalytic oxidation of methane to methanol-a critical assessment. *Angew. Chem., Int. Ed.* **2017**, *56*, 16464−16483.

(15) Periana, R. A.; Mironov, O.; Taube, D.; Bhalla, G.; Jones, C. J. Catalytic, oxidative condensation of CH_4 to CH_3COOH in one step via CH activation. *Science* **2003**, *301*, 814−818.

(16) Li, L.; Fan, S.; Mu, X.; Mi, Z.; Li, C. J. Photoinduced conversion of methane into benzene over GaN nanowires. *J. Am. Chem. Soc.* **2014**, *136*, 7793−7796.

(17) Cook, A. K.; Schimler, S. D.; Matzger, A. J.; Sanford, M. S. Catalyst-controlled selectivity in the C-H borylation of methane and ethane. *Science* **2016**, *351*, 1421−1424.

(18) Smith, K. T.; Berritt, S.; Gonzalez-Moreiras, M.; Ahn, S.; Smith, M. R., 3rd; Baik, M. H.; Mindiola, D. J. Catalytic borylation of methane. *Science* **2016**, *351*, 1424−1427.

(19) Hu, A.; Guo, J. J.; Pan, H.; Zuo, Z. Selective functionalization of methane, ethane, and higher alkanes by cerium photocatalysis. *Science* **2018**, *361*, 668−672.

(20) Cui, X.; Li, H.; Wang, Y.; Hu, Y.; Hua, L.; Li, H.; Han, X.; Liu, Q.; Yang, F.; He, L.; Chen, X.; Li, Q.; Xiao, J.; Deng, D.; Bao, X. Room-temperature methane conversion by graphene-confined single iron atoms. *Chem.* **2018**, *4*, 1902−1910.

(21) Zhang, X.; Huang, Z.; Ferrandon, M.; Yang, D.; Robison, L.; Li, P.; Wang, T. C.; Delferro, M.; Farha, O. K. Catalytic chemoselective functionalization of methane in a metal−organic framework. *Nat. Catal.* **2018**, *1*, 356−362.

(22) Feng, X.; Song, Y.; Li, Z.; Kaufmann, M.; Pi, Y.; Chen, J. S.; Xu, Z.; Li, Z.; Wang, C.; Lin, W. Metal-organic framework stabilizes a low-coordinate iridium complex for catalytic methane borylation. *J. Am. Chem. Soc.* **2019**, *141*, 11196−11203.

(23) Vargaftik, M. N.; Stolarov, I. P.; Moiseev, I. I. Highly selective partial oxidation of methane to methyl trifluoroacetate. *J. Chem. Soc., Chem. Commun.* **1990**, 1049.

(24) Kao, L. C.; Hutson, A. C.; Sen, A. Low-temperature, palladium(II)-catalyzed, solution-phase oxidation of methane to methanol derivative. *J. Am. Chem. Soc.* **1991**, *113*, 700−701.

(25) Periana, R. A.; Taube, D. J.; Gamble, S.; Taube, H.; Satoh, T.; Fujii, H. Platinum catalysts for the high-yield oxidation of methane to a methanol derivative. *Science* **1998**, *280*, 560−564.

(26) Yin, G. C.; Piao, D. G.; Kitamura, T.; Fujiwara, Y. $Cu(OAc)_2$-catalyzed partial oxidation of methane to methyl trifluoroacetate in the liquid phase. *Appl. Organomet. Chem.* **2000**, *14*, 438−442.

(27) Muehlhofer, M.; Strassner, T.; Herrmann, W. A New catalyst systems for the catalytic conversion of methane into methanol. *Angew. Chem., Int. Ed.* **2002**, *41*, 1745−1747.

(28) An, Z.; Pan, X.; Liu, X.; Han, X.; Bao, X. Combined redox couples for catalytic oxidation of methane by dioxygen at low temperatures. *J. Am. Chem. Soc.* **2006**, *128*, 16028−16029.

(29) Meyer, D.; Taige, M. A.; Zeller, A.; Hohlfeld, K.; Ahrens, S.; Strassner, T. Palladium complexes with pyrimidine-functionalized N-heterocyclic carbene ligands: synthesis, structure and catalytic activity. *Organometallics* **2009**, *28*, 2142−2149.

(30) Zimmermann, T.; Soorholtz, M.; Bilke, M.; Schuth, F. Selective methane oxidation catalyzed by platinum salts in oleum at turnover frequencies of large-scale industrial processes. *J. Am. Chem. Soc.* **2016**, *138*, 12395−12400.

(31) Ravi, M.; van Bokhoven, J. A. Homogeneous copper-catalyzed conversion of methane to methyl trifluoroacetate in high yield at low pressure. *ChemCatChem* **2018**, *10*, 2383−2386.

(32) Palkovits, R.; Antonietti, M.; Kuhn, P.; Thomas, A.; Schuth, F. Solid catalysts for the selective low-temperature oxidation of methane to methanol. *Angew. Chem., Int. Ed.* **2009**, *48*, 6909−6912.

(33) Ikuno, T.; Zheng, J.; Vjunov, A.; Sanchez-Sanchez, M.; Ortuno, M. A.; Pahls, D. R.; Fulton, J. L.; Camaioni, D. M.; Li, Z.; Ray, D.; Mehdi, B. L.; Browning, N. D.; Farha, O. K.; Hupp, J. T.; Cramer, C. J.; Gagliardi, L.; Lercher, J. A. Methane oxidation to methanol catalyzed by Cu-Oxo clusters stabilized in NU-1000 metal-organic framework. *J. Am. Chem. Soc.* **2017**, *139*, 10294−10301.

(34) Baek, J.; Rungtaweevoranit, B.; Pei, X.; Park, M.; Fakra, S. C.; Liu, Y. S.; Matheu, R.; Alshmimri, S. A.; Alshehri, S.; Trickett, C. A.; Somorjai, G. A.; Yaghi, O. M. Bioinspired metal-organic framework catalysts for selective methane oxidation to methanol. *J. Am. Chem. Soc.* **2018**, *140*, 18208−18216.

(35) Jin, Z.; Wang, L.; Zuidema, E.; Mondal, K.; Zhang, M.; Zhang, J.; Wang, C.; Meng, X.; Yang, H.; Mesters, C.; Xiao, F. S. Hydrophobic zeolite modification for in situ peroxide formation in methane oxidation to methanol. *Science* **2020**, *367*, 193−197.

(36) Coperet, C. C-H bond activation and organometallic intermediates on isolated metal centers on oxide surfaces. *Chem. Rev.* **2010**, *110*, 656−680.

(37) Olsbye, U.; Svelle, S.; Bjorgen, M.; Beato, P.; Janssens, T. V.; Joensen, F.; Bordiga, S.; Lillerud, K. P. Conversion of methanol to hydrocarbons: how zeolite cavity and pore size controls product selectivity. *Angew. Chem., Int. Ed.* **2012**, *51*, 5810−5831.

(38) Schwach, P.; Pan, X.; Bao, X. Direct conversion of methane to value-added chemicals over heterogeneous catalysts: challenges and prospects. *Chem. Rev.* **2017**, *117*, 8497−8520.

(39) Chen, W.; Kocal, J. A.; Brandvold, T. A.; Bricker, M. L.; Bare, S. R.; Broach, R. W.; Greenlay, N.; Popp, K.; Walenga, J. T.; Yang, S. S.; Low, J. J. Manganese oxide catalyzed methane partial oxidation in trifluoroacetic acid: Catalysis and kinetic analysis. *Catal. Today* **2009**, *140*, 157−161.
(40) Strassner, T.; Ahrens, S.; Muehlhofer, M.; Munz, D.; Zeller, A. Cobalt-Catalyzed Oxidation of Methane to Methyl Trifluoroacetate by Dioxygen. *Eur. J. Inorg. Chem.* **2013**, *2013*, 3659−3663.
(41) Drake, T.; Ji, P.; Lin, W. Site isolation in metal-organic frameworks enables novel transition metal catalysis. *Acc. Chem. Res.* **2018**, *51*, 2129−2138.
(42) Taylor, D.; Dalgarno, S. J.; Xu, Z.; Vilela, F. Conjugated porous polymers: incredibly versatile materials with far-reaching applications. *Chem. Soc. Rev.* **2020**, *49*, 3981−4042.
(43) Phan, A.; Czaja, A. U.; Gándara, F.; Knobler, C. B.; Yaghi, O. M. Metal−organic frameworks of vanadium as catalysts for conversion of methane to acetic acid. *Inorg. Chem.* **2011**, *50*, 7388−7390.
(44) Yang, X. L.; Xie, M. H.; Zou, C.; He, Y.; Chen, B.; O'Keeffe, M.; Wu, C. D. Porous metalloporphyrinic frameworks constructed from metal 5,10,15,20-tetrakis(3,5-biscarboxylphenyl)porphyrin for highly efficient and selective catalytic oxidation of alkylbenzenes. *J. Am. Chem. Soc.* **2012**, *134*, 10638−10645.
(45) Zhang, T.; Manna, K.; Lin, W. Metal-organic frameworks stabilize solution-inaccessible cobalt catalysts for highly efficient broad-scope organic transformations. *J. Am. Chem. Soc.* **2016**, *138*, 3241−3249.
(46) Manna, K.; Ji, P.; Greene, F. X.; Lin, W. Metal-organic framework nodes support single-site magnesium-alkyl catalysts for hydroboration and hydroamination reactions. *J. Am. Chem. Soc.* **2016**, *138*, 7488−7491.
(47) Xiao, D. J.; Oktawiec, J.; Milner, P. J.; Long, J. R. Pore environment effects on catalytic cyclohexane oxidation in expanded Fe_2(dobdc) analogues. *J. Am. Chem. Soc.* **2016**, *138*, 14371−14379.
(48) Huang, N.; Wang, K.; Drake, H.; Cai, P.; Pang, J.; Li, J.; Che, S.; Huang, L.; Wang, Q.; Zhou, H. C. Tailor-Made Pyrazolide-Based Metal-Organic Frameworks for Selective Catalysis. *J. Am. Chem. Soc.* **2018**, *140*, 6383−6390.
(49) Sun, C.; Skorupskii, G.; Dou, J. H.; Wright, A. M.; Dinca, M. Reversible metalation and catalysis with a scorpionate-like metalloligand in a metal-organic framework. *J. Am. Chem. Soc.* **2018**, *140*, 17394−17398.
(50) Cao, C. C.; Chen, C. X.; Wei, Z. W.; Qiu, Q. F.; Zhu, N. X.; Xiong, Y. Y.; Jiang, J. J.; Wang, D.; Su, C. Y. Catalysis through Dynamic Spacer Installation of Multivariate Functionalities in Metal-Organic Frameworks. *J. Am. Chem. Soc.* **2019**, *141*, 2589−2593.
(51) Zhang, Y.; Riduan, S. N. Functional porous organic polymers for heterogeneous catalysis. *Chem. Soc. Rev.* **2012**, *41*, 2083−2094.
(52) Sun, Q.; Dai, Z.; Liu, X.; Sheng, N.; Deng, F.; Meng, X.; Xiao, F. S. Highly efficient heterogeneous hydroformylation over Rh-metalated porous organic polymers: synergistic effect of high ligand concentration and flexible framework. *J. Am. Chem. Soc.* **2015**, *137*, 5204−5209.
(53) Tanabe, K. K.; Ferrandon, M. S.; Siladke, N. A.; Kraft, S. J.; Zhang, G.; Niklas, J.; Poluektov, O. G.; Lopykinski, S. J.; Bunel, E. E.; Krause, T. R.; Miller, J. T.; Hock, A. S.; Nguyen, S. T. Discovery of highly selective alkyne semihydrogenation catalysts based on first-row transition-metallated porous organic polymers. *Angew. Chem., Int. Ed.* **2014**, *53*, 12055−12058.
(54) Iwai, T.; Harada, T.; Hara, K.; Sawamura, M. Threefold Cross-Linked Polystyrene-Triphenylphosphane Hybrids: Mono-P-Ligating Behavior and Catalytic Applications for Aryl Chloride Cross-Coupling and C(sp^3)−H Borylation. *Angew. Chem., Int. Ed.* **2013**, *52*, 12322−12326.
(55) Yang, Z.; Chen, H.; Li, B.; Guo, W.; Jie, K.; Sun, Y.; Jiang, D. E.; Popovs, I.; Dai, S. Topotactic synthesis of phosphabenzene-functionalized porous organic polymers: efficient ligands in CO_2 conversion. *Angew. Chem., Int. Ed.* **2019**, *58*, 13763−13767.
(56) Kramer, S.; Bennedsen, N. R.; Kegnæs, S. Porous organic polymers containing active metal centers as catalysts for synthetic organic chemistry. *ACS Catal.* **2018**, *8*, 6961−6982.
(57) Zhang, Y.; Zhang, Y.; Sun, Y. L.; Du, X.; Shi, J. Y.; Wang, W. D.; Wang, W. 4-(N,N-dimethylamino)pyridine-embedded nanoporous conjugated polymer as a highly active heterogeneous organocatalyst. *Chem. - Eur. J.* **2012**, *18*, 6328−6334.
(58) Li, W. H.; Li, C. Y.; Li, Y.; Tang, H. T.; Wang, H. S.; Pan, Y. M.; Ding, Y. J. Palladium-metalated porous organic polymers as recyclable catalysts for chemoselective decarbonylation of aldehydes. *Chem. Commun.* **2018**, *54*, 8446−8449.
(59) Huangfu, Y.; Sun, Q.; Pan, S.; Meng, X.; Xiao, F.-S. Porous polymerized organocatalysts rationally synthesized from the corresponding vinyl-functionalized monomers as efficient heterogeneous catalysts. *ACS Catal.* **2015**, *5*, 1556−1559.
(60) Eddaoudi, M.; Kim, J.; Rosi, N.; Vodak, D.; Wachter, J.; O'Keeffe, M.; Yaghi, O. M. Systematic design of pore size and functionality in isoreticular MOFs and their application in methane storage. *Science* **2002**, *295*, 469−472.
(61) Murray, L. J.; Dinca, M.; Long, J. R. Hydrogen storage in metal-organic frameworks. *Chem. Soc. Rev.* **2009**, *38*, 1294−1314.
(62) Li, J. R.; Kuppler, R. J.; Zhou, H. C. Selective gas adsorption and separation in metal-organic frameworks. *Chem. Soc. Rev.* **2009**, *38*, 1477−1504.
(63) Puthiaraj, P.; Cho, S.-M.; Lee, Y.-R.; Ahn, W.-S. Microporous covalent triazine polymers: efficient Friedel−Crafts synthesis and adsorption/storage of CO_2 and CH_4. *J. Mater. Chem. A* **2015**, *3*, 6792−6797.
(64) Liu, G.; Wang, Y.; Shen, C.; Ju, Z.; Yuan, D. A facile synthesis of microporous organic polymers for efficient gas storage and separation. *J. Mater. Chem. A* **2015**, *3*, 3051−3058.
(65) Puthiaraj, P.; Kim, S.-S.; Ahn, W.-S. Covalent triazine polymers using a cyanuric chloride precursor via Friedel−Crafts reaction for CO_2 adsorption/separation. *Chem. Eng. J.* **2016**, *283*, 184−192.
(66) Li, B.; Guan, Z.; Wang, W.; Yang, X.; Hu, J.; Tan, B.; Li, T. Highly dispersed pd catalyst locked in knitting aryl network polymers for Suzuki-Miyaura coupling reactions of aryl chlorides in aqueous media. *Adv. Mater.* **2012**, *24*, 3390−3395.

https://dx.doi.org/10.1021/acscatal.0c05205
ACS Catal. 2021, 11, 1008−1013